Noname manuscript No.
(will be inserted by the editor)

A Closed NPZ Model with Delayed Nutrient Recycling

Matt Kloosterman · **Sue Ann Campbell** ·
Francis J. Poulin

Received: date / Accepted: date

Abstract We consider a closed Nutrient-Phytoplankton-Zooplankton (NPZ) model that allows for a delay in the nutrient recycling. A delay-dependent conservation law allows us to quantify the total biomass in the system. With this, we can investigate how a planktonic ecosystem is affected by the quantity of biomass it contains and by the properties of the delay distribution. The quantity of biomass and the length of the delay play an significant role in determining the existence of equilibrium solutions, since a sufficiently small amount of biomass or a long enough delay can lead to the extinction of a species. Furthermore, the quantity of biomass and length of delay are important since a small change in either can change the stability of an equilibrium solution. We explore these effects for a variety of delay distributions using both analytical and numerical techniques, and verify results with simulations.

Keywords Plankton · Delay · Nutrient Recycling · Closed ecosystem

Mathematics Subject Classification (2000) 37N25

Matt Kloosterman
Department of Applied Mathematics, University of Waterloo, Waterloo, ON, Canada N2L 3G1
Tel.: (519) 888-4567 ext. 33471
Fax: (519) 746-4319
E-mail: mklooste@uwaterloo.ca

Sue Ann Campbell
Department of Applied Mathematics, University of Waterloo, Waterloo, ON, Canada N2L 3G1
Tel.: (519) 888-4567 ext. 35461
Fax: (519) 746-4319
E-mail: sacampbell@uwaterloo.ca

Francis Poulin
Department of Applied Mathematics, University of Waterloo, Waterloo, ON, Canada N2L 3G1
Tel.: (519) 888-4567 ext. 32637
Fax: (519) 746-4319
E-mail: fpoulin@uwaterloo.ca

1 Introduction

Plankton are at the bottom of most oceanic food webs, and therefore it is important to understand the dynamics of planktonic ecosystems. Typically, the first trophic level consists of phytoplankton, which uptake nutrient through photosynthesis. The second trophic level is formed by zooplankton, which feed on phytoplankton. It is convenient to study the interaction of phytoplankton and zooplankton using a predator-prey based model. These models can range from very simple Lotka-Volterra models (Murray, 1989) to very complicated equations that consist of not only reaction type terms but also advection, diffusion and even size-structure. Typically, the more complicated the model, the more parameters need to be chosen, and, consequently, overly-complex models are harder to learn from than simpler ones.

Using a three compartment Nutrient-Phytoplankton-Zooplankton (NPZ) model, we focus on how the existence and stability of equilibrium solutions depend on two properties: (1) the total biomass in the system (measured in dissolved nitrogen), and (2) the delay that characterizes the recycling of nutrients.

In order to investigate the effects of the total biomass, we assume a closed system where nutrient is conserved for all time. Consequently, there will be a fixed constant, N_T, that represents the amount of dissolved nitrogen in the system in time. A good introduction to NPZ models in this form is given in Franks (2002), and has been studied in Gentleman and Neuheimer (2008) and Wroblewski et al (1988) and references within. Other closed ecosystem models can be found in Ulanowicz (1972) and Kmet (1996).

An alternative to having a closed system would be to have one where there are sources and sinks, which are typically referred to as washout rates, where biomass flows in and out of the system at some rate. These are often used in chemostat models. Our model may be seen as the limiting case where the washout rate tends to zero. In an open system, the total biomass in the system usually tends to the concentration flowing in, while without a washout rate the total biomass is fixed by the initial condition. The washout rate may be important in some ecosystems, but can be ignored when considering a large, self-contained ecosystem. An example of this is a closed lake.

In Beretta et al (1990), the authors state that since the washout rate is much smaller in a natural system than in a chemostat situation, nutrient recycling must be considered. When plankton die, the remains are not immediately ready to be uptaken by phytoplankton; there is an interval of time during which nutrient recycling takes place. The length and other characteristic features of the delay can affect stability, and we will analyze this along with the total nutrient in the system. This type of delay has been studied frequently in chemostat-type models, (He and Ruan, 1998; Ruan, 1998, 2001). However, the inclusion of delay in a closed system brings forth an alternative structure in the governing equations that requires a different perspective that has received much less attention. The amount of biomass in a system with washout rates is characterized by an explicit parameter: the concentration of nutrient flowing into the system. In the closed model that we will consider, the total biomass is not an explicit parameter found in the equations, but rather is implicit within the initial conditions.

2 Model

The dynamics of our planktonic ecosystem model are governed by a three compartment NPZ model. Respectively, these compartments represent the dissolved nutrient, the amount of phytoplankton, and the amount of zooplankton. Each compartment is measured by its content of the limiting biomass, which is usually nitrogen. Following the lead of Franks (2002), we assume that five basic processes govern the ecosystem: (1) the phytoplankton nutrient uptake, (2) the zooplankton grazing on phytoplankton, (3) the death of phytoplankton, (4) the death of zooplankton, and (5) nutrient recycling. We assume that there is a delay in nutrient recycling. The state equations then take the following form:

$$\begin{aligned}\frac{dN(t)}{dt} =& \lambda \int_0^\infty P(t-u)\eta(u)\,du + \delta \int_0^\infty Z(t-u)\eta(u)\,du \\ &+ (1-\gamma)g \int_0^\infty Z(t-u)h(P(t-u))\eta(u)\,du - \mu P(t) f(N(t)), \qquad (1a)\\ \frac{dP(t)}{dt} =& \mu P(t) f(N(t)) - gZ(t)h(P(t)) - \lambda P(t), \qquad (1b)\\ \frac{dZ(t)}{dt} =& \gamma g Z(t) h(P(t)) - \delta Z(t). \qquad (1c)\end{aligned}$$

Here, phytoplankton reproduce at a rate proportional to their population size and to a general function of the available nutrient, $f(N)$. Similarly, zooplankton reproduce at a rate proportional to their population size and to a function of the available phytoplankton, $h(P)$. The parameter, γ, sets the ratio of the biomass lost from the phytoplankton variable because of grazing and the biomass gained in the zooplankton variable. The rest is returned to the dissolved nutrient variable. We assume the death rates are proportional to the population sizes, and all the nutrient then returns to the dissolved nutrient field. This recycling of nutrient is not necessarily instantaneous, but occurs after some delay according to the distribution η, which is non-negative and normalized so that $\int_0^\infty \eta(u)\,du = 1$.

The functional form of the phytoplankton nutrient uptake, $f(N) \in C^2$, will be assumed to have the following properties:

$$f(0) = 0, \quad f'(N) > 0, \quad f''(N) < 0, \quad \lim_{N\to\infty} f(N) = 1. \qquad (2)$$

The most common functional response (Franks, 2002) is the Michaelis-Menten formulation:

$$f(N) = \frac{N}{N+k}, \qquad (3)$$

which is one choice that satisfies these properties.

The functional responses of the zooplankton grazing on phytoplankton are usually characterized by a particular type, as described in Holling (1966). A Type I response depends linearly on the population density (e.g. $h(P) = aP$). A Type II response has a “negatively accelerated rise to a plateau” (Holling, 1966) and a Type III response is

sigmoidal shaped. We will focus on the latter two and assume the following properties:

$$h(0) = 0, \quad h'(P) > 0, \quad \lim_{P\to\infty} h(P) = 1. \tag{4}$$

Similar properties are found in Ruan (2001) and Hale and Somolinos (1983). We will also assume $h \in C^1$. The particular choice of how zooplankton graze on phytoplankton is a very important aspect of the model, as it has a significant impact on the stability of the ecosystem (Gentleman and Neuheimer, 2008).

The closure term δZ incorporates not only the natural death of zooplankton, but also the effects of higher predation. Consequently, it is often taken to be quadratic (δZ^2), which approximates a Type III response of predation, while a linear terms is better at approximating a Type II response. An important feature (Franks, 2002) is that a quadratic closure term makes the system much more stable. However, it is much easier to analyze the existence of equilibrium solutions using a linear closure term since the rate of change of zooplankton can be made zero independently of the value of Z. Furthermore, intuitively it seems the closure term should be linear as the zooplankton population tends to zero, as we might expect predation to be negligible compared to the natural death process in this limit. Because of this, in Caswell and Neubert (1998) they use a closure term with both a linear and nonlinear part. For simplicity we will choose a linear closure term, and will perhaps address in future work the impact of quadratic closure schemes.

The reason for the delay in the nutrient recycling is that there is a period of decomposition when a plankter dies, so treating this as an instantaneous process differs from the true dynamics. This recycling comes from three processes: the phytoplankton deaths, the zooplankton deaths, and the inefficiency of the grazing. As a starting point, it will be assumed that these three processes have the same delay distribution. This is not true in reality, but the effect that the delay has on the system would become much harder to understand if we were to consider three different distributions, so it is worth seeing what results can be obtained from the assumption that they are all the same. In future work it would be of interest to consider separate delay distributions but that is beyond the scope of this work.

While it is true that in reality there must necessarily exist an upper bound on the length of delay, it is sometimes convenient to allow for unbounded delay distributions. While we will consider distributions with bounded delay, we will not restrict our attention to them completely.

We can view the distribution of delays, $\eta(u)$, as the probability that an amount of nutrient will take time u to be recycled. If there is a large range of possible times over which an amount of nutrient is recycled, then the distribution is wide with large variance. On the other hand, if the nutrient recycling always takes roughly the same amount of time, the distribution is narrow with small variance. Furthermore, one could assume a discrete delay, where the recycling takes a fixed amount of time with 100% probability. This distribution can be seen as the limit of a sequence of distributions whose variances become smaller and smaller. In this case, the distribution is $\eta(u) = \delta(u-\tau)$, where $\delta(x)$ is the Dirac delta distribution. This then leads to the

equations

$$\frac{dN(t)}{dt} = \lambda P(t-\tau) + \delta Z(t-\tau) + (1-\gamma) g Z(t-\tau) h(P(t-\tau)) - \mu P(t) f(N(t)), \tag{5a}$$

$$\frac{dP(t)}{dt} = \mu P(t) f(N(t)) - g Z(t) h(P(t)) - \lambda P(t), \tag{5b}$$

$$\frac{dZ(t)}{dt} = \gamma g Z(t) h(P(t)) - \delta Z(t). \tag{5c}$$

An NPZD model is a variant of an NPZ model that includes an additional variable: detritus, which represents the faecal pellets of zooplankton and dead phytoplankton and zooplankton. As we now show, an NPZD model can be equivalent to an NPZ model with delayed nutrient recycling. This is a result of the common "linear chain trick," although the context here is special in that the extra variable, detritus, has a clear physical meaning. Denoting the detritus as D, a typical NPZD model takes the form:

$$\frac{dN}{dt} = \alpha D - \mu P f(N), \tag{6a}$$

$$\frac{dP}{dt} = \mu P f(N) - g Z h(P) - \lambda P, \tag{6b}$$

$$\frac{dZ}{dt} = \gamma g Z h(P) - \delta Z, \tag{6c}$$

$$\frac{dD}{dt} = \lambda P + \delta Z + (1-\gamma) g Z h(P) - \alpha D. \tag{6d}$$

This system is equivalent to (1) if we choose $\eta(u) = \alpha e^{-\alpha u}$, which can be seen by letting

$$D(t) = \frac{1}{\alpha} \int_0^\infty [\lambda P(t-u) + \delta Z(t-u) + (1-\gamma) g Z(t-u) h(P(t-u))] \eta(u)\, du.$$

A detritus model applied to an open ecosystem was analyzed in Edwards (2001). By studying systems with general delay distributions, we are including systems such as (6) as a special case in our analysis.

2.1 Mathematical Properties

We now consider some mathematical properties of the model (1). First, since the model is closed, there is no biomass lost or gained in the ecosystem. Consequently,

there is a conservation law, which is obtained by adding the equations in (1) to yield

$$\begin{aligned}
&\frac{d}{dt}[N(t)+P(t)+Z(t)]\\
&=\int_0^\infty [\lambda P(t-u)+\delta Z(t-u)+(1-\gamma)gZ(t-u)h(P(t-u))]\eta(u)\,du\\
&\quad-\lambda P(t)-\delta Z(t)-(1-\gamma)gZ(t)h(P(t)),\\
&=\int_0^\infty [\lambda P(t-u)+\delta Z(t-u)+(1-\gamma)gZ(t-u)h(P(t-u))\\
&\quad-\lambda P(t)-\delta Z(t)-(1-\gamma)gZ(t)h(P(t))]\eta(u)\,du,\\
&=-\frac{d}{dt}\int_0^\infty\int_{t-u}^t [\lambda P(v)+\delta Z(v)+(1-\gamma)gZ(v)h(P(v))]\eta(u)\,dv\,du,
\end{aligned}$$

so that the quantity

$$\begin{aligned}
N_T &= N(t)+P(t)+Z(t)\\
&\quad+\int_0^\infty\int_{t-u}^t [\lambda P(v)+\delta Z(v)+(1-\gamma)gZ(v)h(P(v))]\eta(u)\,dv\,du
\end{aligned}\tag{7}$$

is conserved in time. The total biomass in the system, N_T, is thus given by the sum of the nutrient in the three compartments plus that in the process of being recycled. If we ignore the delay (set $\eta(u)=\delta(u)$), we recover the simpler conservation law $N_T = N(t)+P(t)+Z(t)$ found in Franks et al (1986).

Next, we write the model (1) in the general form

$$\frac{dx(t)}{dt} = F(x_t) \qquad \text{for } t>0, \tag{8}$$

where $x=(N,P,Z)^T$ and

$$x_t(\theta) = x(t+\theta) \qquad \text{for } \theta \le 0.$$

An appropriate initial condition is then

$$x_0 = \phi. \tag{9}$$

Since (8) is a delay differential equation with infinite delay, an appropriate phase space for the problem is $C_{0,\rho}((-\infty,0],\mathbb{R}^3)$ where $\rho>0$ (Hino et al, 1991; Kolmanovskii and Myshkis, 1999; Diekmann and Gyllenberg, 2012). This is the Banach space of functions $\psi:(-\infty,0]\to\mathbb{R}^3$ such that $e^{\rho\theta}\psi(\theta)$ is continuous and

$$\lim_{\theta\to-\infty} e^{\rho\theta}\psi(\theta)=0.$$

This space is equipped with the norm

$$\|\psi\|_{\infty,\rho} = \sup_{\theta\le 0} e^{\rho\theta}\psi(\theta).$$

Table 1 Parameter values used for all computations

Parameter	Value
μ	5.9 day^{-1}
λ	0.017 day^{-1}
g	7 day^{-1}
γ	0.7
δ	0.17 day^{-1}
$f(N)$	$\frac{N}{N+k}$
$h(P)$	$\frac{P}{P+K}$
k	1.0μM
K	1.0μM

Then, $F : C_{0,\rho}((-\infty,0],\mathbb{R}^3) \to \mathbb{R}^3$, and with the above assumptions on f and h, for any $\phi \in C_{0,\rho}((-\infty,0],\mathbb{R}^3)$ there exists a unique solution. In this phase space, we need the following condition to hold:

$$\int_0^\infty e^{\rho u}\eta(u)\,du < \infty. \tag{10}$$

For the purposes of numerical computations, the values in Table 1 will be used. These were taken from Poulin and Franks (2010).

3 Equilibrium Solutions

Substituting a time-independent solution, $(N(t),P(t),Z(t)) = (N^*,P^*,Z^*)$ for all $t \in \mathbb{R}$, into (1), we see that the system is in equilibrium if the following equations are satisfied:

$$\mu P^* f(N^*) - gZ^* h(P^*) - \lambda P^* = 0, \tag{11a}$$

$$\gamma g Z^* h(P^*) - \delta Z^* = 0. \tag{11b}$$

If these two equations hold, then the growth rates of each variable is zero, regardless of the delay distribution. Hence, we have one degree of freedom when finding a steady state solution. That is, equilibrium solutions come in sets due to the conservation law (7). However, we can consider the total biomass, N_T, to be a fixed parameter of the system. Then an equilibrium solution (N^*,P^*,Z^*) must also satisfy

$$N_T = N^* + P^* + Z^* + [\lambda P^* + \delta Z^* + (1-\gamma)gZ^* h(P^*)]\tau, \tag{12}$$

where τ is the mean delay:

$$\tau = \int_0^\infty u\eta(u)\,du.$$

From the conservation law (12), we see a relationship between the total biomass and the length of delay. If we consider the equilibrium solution as given, the total nutrient is a linear function of the mean delay. This is because a longer delay means that at a given time there is more nutrient in the process of being recycled, so there is

necessarily more nutrient in the system. Alternatively, we can consider the total nutrient to be fixed, and the equilibrium solutions to be functions of the mean delay and total nutrient. While it is often true that the equilibrium solutions of delay differential equations do not depend on the delay, if the total nutrient is a fixed parameter then the equilibrium solutions in our model do indeed have delay dependence. Increasing the delay then decreases the equilibrium values, since at a given time a larger portion of the total nutrient is in the process of being recycled.

There are three types of equilibrium solutions. Since the state variables represent physical quantities, only non-negative solutions are meaningful, therefore an equilibrium solution does not exist if it has negative values.

The first equilibrium solution is the trivial equilibrium. Setting $P = Z = 0$ satisfies (11a) and (11b). Then, from the conservation law, we get that $N^* = N_T$. This steady state solution will be referred to as $(N_T, 0, 0)$, or simply as the trivial solution. Biologically this represents the states where there is no life in the ecosystem.

The second type of equilibrium is in the form $(\hat{N}, \hat{P}, 0)$, with $\hat{N} > 0$ and $\hat{P} > 0$. By setting $Z = 0$, (11b) is satisfied. A necessary condition for (11a) to be satisfied is

$$\mu > \lambda, \tag{13}$$

which means the maximum growth rate of phytoplankton must be greater than its death rate. If this is true, then equation (11a) is satisfied by setting $\hat{N} = f^{-1}(\lambda/\mu)$. Since f is an increasing function with $0 \leq f(N) < 1$, this value is well-defined and unique if $\mu > \lambda$. From the conservation law (12), we get

$$\hat{P} = \frac{N_T - f^{-1}(\lambda/\mu)}{1 + \lambda\tau}. \tag{14}$$

Thus, this equilibrium point exists if and only if $N_T > N_{T1}$, where

$$N_{T1} = f^{-1}\left(\frac{\lambda}{\mu}\right). \tag{15}$$

Finally, we now consider the equilibrium point of type (N^*, P^*, Z^*), with all three components positive. A necessary condition for (11b) to be satisfied with $Z^* \neq 0$ is

$$\gamma g > \delta, \tag{16}$$

which means that the maximum growth rate of the zooplankton must be greater than its death rate. If (16) is satisfied, then

$$P^* = h^{-1}\left(\frac{\delta}{\gamma g}\right). \tag{17}$$

Then from (11a):

$$Z^* = \frac{\gamma P^*}{\delta}[\mu f(N^*) - \lambda]. \tag{18}$$

Now N^* must satisfy the conservation law (12), which leads to the implicit expression for N^*:

$$N_T = N^* + h^{-1}\left(\frac{\delta}{\gamma g}\right)\left[1 - \frac{\gamma\lambda}{\delta} + \left(\frac{\gamma}{\delta} + \tau\right)\mu f(N^*)\right]. \tag{19}$$

Note that N_T is a continuous increasing function of N^*. Setting N^* to $f^{-1}(\lambda/\mu)$, we see that $N_T = N_{T2}$, where

$$N_{T2} = f^{-1}\left(\frac{\lambda}{\mu}\right) + (1+\lambda\tau)h^{-1}\left(\frac{\delta}{\gamma g}\right). \tag{20}$$

Again, since h is an increasing function, this value is unique and well-defined if $\gamma g > \delta$, which we assume to be true for the same reason we assume $\mu > \lambda$. If $N_T > N_{T2}$, then $N^* > f^{-1}(\lambda/\mu)$, which implies $Z^* > 0$. This shows the equilibrium point exists if $N_T > N_{T2}$. Conversely, $Z^* < 0$ if $N_T < N_{T2}$, so then the equilibrium point does not exist.

The uniqueness of each type of equilibrium point follows from the fact that f and h are increasing functions.

In Levin et al (1977), the authors state that if the prey population in the absence of predators is large enough to support predators, in our case zooplankton, then the positive equilibrium exists, which is precisely the case here. Indeed, if $\hat{P} > P^*$, then there is enough nutrient to support both populations. This equilibrium solution is more ecologically diverse and also more relevant to what is observed in the world's oceans and lakes.

In the following sections, we will assume the conditions (13) and (16) are satisfied, and focus on the effects of the total biomass, N_T, and delay on the stability of the equilibria.

4 Characteristic Equation

The differentiability conditions on f and h in (2) and (4) with the condition on η in (10) assure that F in (8) is Fréchet differentiable. The Fréchet derivative at an equilibrium solution, $x^* = (N^*, P^*, Z^*)^T$, is

$$DF(x^*)\psi = A_0\psi(0) + A_1\int_0^\infty \psi(-u)\eta(u)\,du, \tag{21}$$

where

$$A_0 = \begin{pmatrix} -\mu P^* a & -\mu c & 0 \\ \mu P^* a & \mu c - \lambda - gZ^* b & -gd \\ 0 & \gamma g Z^* b & \gamma g d - \delta \end{pmatrix}, \tag{22}$$

$$A_1 = \begin{pmatrix} 0 & \lambda + (1-\gamma)gZ^* b & \delta + (1-\gamma)gd \\ 0 & 0 & 0 \\ 0 & 0 & 0 \end{pmatrix}. \tag{23}$$

and $a = f'(N^*), b = h'(P^*), c = f(N^*)$, and $d = h(P^*)$.

The linearized equation around an equilibrium solution is then:

$$\frac{dx(t)}{dt} = DF(x^*)(x_t - x^*), \tag{24}$$

$$= A_0(x(t) - x^*) + A_1\int_0^\infty (x(t-u) - x^*)\eta(u)\,du. \tag{25}$$

Taking the Laplace transform of (24) gives the characteristic equation:

$$\det[sI - A_0 - A_1\hat{\eta}(s)] = 0, \tag{26}$$

where $\hat{\eta}$ is the Laplace transform of η:

$$\hat{\eta}(s) = \int_0^\infty e^{-su}\eta(u)\,du. \tag{27}$$

The equilibrium solution is locally asymptotically stable if all the roots s that solve $\det(sI - A_0 - A_1\hat{\eta}(s)) = 0$ have negative real parts and unstable if there is at least one root with positive real part (Diekmann and Gyllenberg, 2012).

Note that if we add all the rows of A_0 with all the rows of A_1 we obtain $(0,0,0)$, and hence $s = 0$ is always a solution to the characteristic equation, since $\hat{\eta}(0) = 1$. Thus, to determine the stability of any equilibrium solution, one must consider the center manifold associated with this zero eigenvalue. In the case where the system has bounded delay it can be shown that this center manifold is simply the curve of equilibrium solutions that can be parameterized by the total biomass. This is because the zero eigenvalue is a consequence of the conservation law obeyed by the system. As a result, if all the other eigenvalues have negative real parts, then this manifold is locally attracting, meaning initial conditions that are sufficiently close to the chosen equilibrium will asymptotically go towards a nearby point on the line of equilibria. In particular, the solution will approach the equilibrium solution with the total biomass that is determined by the initial condition. This makes equilibrium solutions stable, but not asymptotically stable. While center manifold theory has not yet been developed for the case where the delay is infinite, we will assume that it is true that an equilibrium solution is stable if the zero eigenvalue caused by the conservation law is the only root with nonnegative real part.

We will now consider the stability of each of the three types of equilibrium points. Our investigation will begin with the system without delay ($\eta(u) = \delta(u)$), and then will continue with non-zero delays.

5 Stability of Solutions without Delay

Much of the work in this section has been done elsewhere, but for completeness we present the results here, as the results for the system with delay depend on those for the system without. We discuss now how the quantity of biomass affects the stability of the equilibrium solutions.

With no delay, the system becomes

$$\frac{dN}{dt} = \lambda P + \delta Z + (1-\gamma)gZh(P) - \mu P f(N), \tag{28a}$$

$$\frac{dP}{dt} = \mu P f(N) - gZh(P) - \lambda P, \tag{28b}$$

$$\frac{dZ}{dt} = \gamma gZh(P) - \delta Z. \tag{28c}$$

Since the conservation law yields $N_T = N(t) + P(t) + Z(t)$, we can substitute $N = N_T - P - Z$ into equation (28b) and remove equation (28a). Then we have the following reduced system:

$$\frac{dP}{dt} = \mu P f(N_T - P - Z) - gZh(P) - \lambda P \tag{29a}$$

$$\frac{dZ}{dt} = \gamma gZh(P) - \delta Z. \tag{29b}$$

Then, given a solution, $P(t)$ and $Z(t)$, we can determine the amount of dissolved nutrient via $N(t) = N_T - P(t) - Z(t)$. If an equilibrium point of the reduced system is asymptotically stable, then the corresponding equilibrium point of the full system is stable. This is because the reduced system has the total nutrient fixed for all initial conditions, while in the full system the total nutrient varies for initial conditions within a neighbourhood of an equilibrium point.

We will denote the phase space as $D = \{(P,Z) : P \geq 0, Z \geq 0, P + Z \leq N_T\}$. This space is positively invariant, which follows from the invariance of the axes, and the fact that $\frac{d}{dt}(P+Z)$ is negative on the line $P + Z = N_T$.

The equilibrium points of the reduced system are the same as those for the full system, but with the N component discarded. The trivial equilibrium of the reduced system becomes $(0,0)$.

Proposition 1 *If $N_T < N_{T1}$ (if the equilibrium $(\hat{P},0)$ does not exist), then the equilibrium solution $(0,0)$ of system (29) is globally asymptotically stable on D.*

Proof Linearizing around this point yields the Jacobian matrix

$$\begin{pmatrix} \mu f(N_T) - \lambda & 0 \\ 0 & -\delta \end{pmatrix}. \tag{30}$$

Here, the eigenvalues are simply the entries on the diagonal. Therefore this point is asymptotically stable if $\mu f(N_T) - \lambda < 0$. Equivalently, this point is asymptotically stable if $N_T < N_{T1}$, where N_{T1} is given in (15). Furthermore, since this is the only equilibrium in D, and it occurs on the boundary, there are no periodic orbits in D. Therefore, this equilibrium is globally asymptotically stable on D. □

This means that if there is not sufficient nutrient to sustain the phytoplankton population, then both phytoplankton and zooplankton become extinct. Furthermore, recall that asymptotic stability of $(0,0)$ in system (29) implies stability of $(N_T,0,0)$ in (28).

Proposition 2 *If $N_{T1} < N_T < N_{T2}$ (if the equilibrium $(\hat{P},0)$ exists, but (P^*,Z^*) does not), then the equilibrium solution $(\hat{P},0)$ of system (29) is globally asymptotically stable on D, except for the Z axis.*

Proof From the linearization of $(0,0)$, $N_{T1} < N_T$ implies that $(0,0)$ is unstable. Linearizing around $(\hat{P},0)$ yields the Jacobian matrix

$$\begin{pmatrix} -\mu\hat{P}f'(N_T - \hat{P}) & -\mu\hat{P}f'(N_T - \hat{P}) - gh(\hat{P}) \\ 0 & \gamma gh(\hat{P}) - \delta \end{pmatrix}. \tag{31}$$

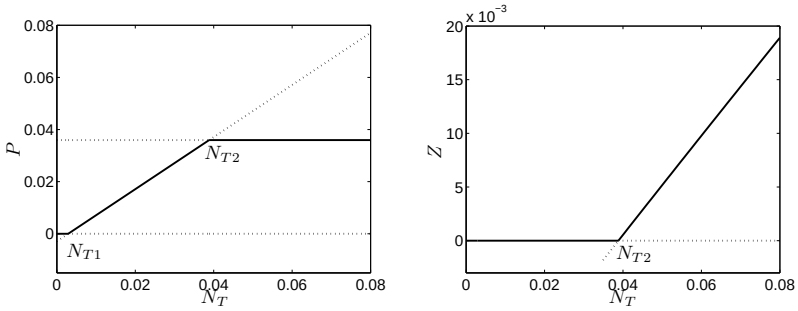

Fig. 1 Equilibrium values of phytoplankton and zooplankton as a function of total nutrient. The solid lines represent asymptotically stable points, while the dotted lines show unstable points

Again, the eigenvalues are simply the diagonal entries. The first eigenvalue is negative since f is increasing. Since we assume that $\delta < \gamma g$, the second eigenvalue is negative if and only if $\hat{P} < h^{-1}(\delta/\gamma g)$. This condition is met if $N_T < N_{T2}$, where N_{T2} is given in (20) with $\tau = 0$. Furthermore, since there are no equilibrium points on the interior of D, there are no periodic orbits, so $(\hat{P}, 0)$ globally attracts all trajectories, except those on the Z axis, which obviously go to the origin. □

Therefore, if there are enough nutrients to sustain the phytoplankton population, but not the zooplankton population as well, the zooplankton becomes extinct, while the phytoplankton persist. Since $\hat{P}$ is positive only if the zero solution is unstable, if we increase the total nutrient past N_{T1}, this equilibrium would exist as soon as the trivial equilibrium becomes unstable.

We now consider the positive equilibrium. Linearizing around (P^*, Z^*), the following Jacobian matrix is obtained:

$$\begin{pmatrix} \frac{\delta Z^*}{\gamma P^*} - \mu P^* a - gbZ^* & -\mu P^* a - \frac{\delta}{\gamma} \\ \gamma gbZ^* & 0 \end{pmatrix}, \tag{32}$$

where $a = f'(N_T - P^* - Z^*)$ and $b = h'(P^*)$. These values are both positive since f and h are increasing functions.

Defining T as the trace and D as the determinant of the matrix, it can easily be seen that the equilibrium solution is asymptotically stable if and only if $T < 0$ and $D > 0$. It is easy to see that $D > 0$. Thus, stability depends on the value of the trace:

$$T = \frac{\delta Z^*}{\gamma P^*} - \mu P^* a - gbZ^* = gZ^* \left(\frac{h(P^*)}{P^*} - h'(P^*) \right) - \mu P^* a. \tag{33}$$

Immediately, we can see that for sufficiently small Z^* the trace is negative and (P^*, Z^*) is therefore asymptotically stable. Since the equilibrium (P^*, Z^*) exists if $N_T > N_{T2}$, if we increase the total nutrient past N_{T2}, the equilibrium $(\hat{P}, 0)$ becomes unstable as soon as (P^*, Z^*) exists and is stable.

It can be seen that N_{T1} and N_{T2} are transcritical bifurcation points, where solution branches intersect and the stability of each branch changes at the intersection. Using

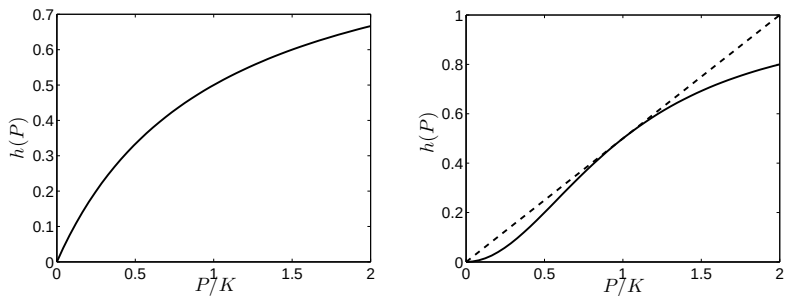

Fig. 2 A Type II functional response (left) in the form $h(P) = \frac{P}{P+K}$ and a Type III functional response (right) in the form $h(P) = \frac{P^2}{P^2+K^2}$. A sufficient condition for stability for this Type III response is that $P^* \leq K$, which means that $h'(P^*) \geq h(P^*)/P^*$. Equivalently, $\delta/\gamma g$ should be less than 1/2

the parameter values in Table 1, Figure 1 shows the equilibrium values of P and Z as a function of total nutrient N_T, and demonstrates the stability changes.

To look for further bifurcations we consider the sign of (33). If $h'(P^*) \geq h(P^*)/P^*$, the equilibrium point is always stable. This condition says that the slope of the secant line from the origin to the point on the graph at the equilibrium point must be less than or equal to the slope of the tangent line at the equilibrium. In Gentleman and Neuheimer (2008), the authors use this idea to argue that a Type III zooplankton grazing response is more stable than Type II. If h is a Type II response, the condition $h'(P^*) \geq h(P^*)/P^*$ is never true, but if it is of Type III, then this condition can be satisfied for P^* below some critical value. This critical value is the value of P where a line through the origin intersects $h(P)$ tangentially. Figure 2 illustrates this idea.

We now investigate the case where $h'(P^*) < h(P^*)/P^*$, as is the case in Type II responses and in Type III responses where $\delta/\gamma g$ is sufficiently close to 1. If $N_T = N_{T2}$, then $Z^* = 0$ and $T < 0$. Thus we conclude that if N_T is sufficiently close to, and greater than, N_{T2}, we have stability. The following proposition then shows how the stability is affected as N_T is increased from N_{T2}.

Proposition 3 *If $h'(P^*) < h(P^*)/P^*$, then there exists a unique value of total nutrient, $N_{T3} > N_{T2}$, such that the point (P^*, Z^*) is asymptotically stable if $N_{T2} < N_T < N_{T3}$ and unstable if $N_T > N_{T3}$.*

Proof Recall that (P^*, Z^*) is asymptotically stable if $T < 0$, and unstable if $T > 0$ where T is the trace in (33). Let $T = T(N_T)$. We will prove the existence of a unique N_{T3} such that $T(N_{T3}) = 0$. Note that P^* and thus b are independent of N_T. However, Z^* and therefore a are functions of N_T. Taking the limit as N_T goes to infinity, and noting that $Z^* \to \gamma P^*(\mu - \lambda)/\delta$ and $a \to 0$ in this limit yields the result

$$T_{max} = \frac{\gamma g}{\delta} P^*(\mu - \lambda)\left(\frac{h(P^*)}{P^*} - h'(P^*)\right) > 0, \tag{34}$$

since $\mu - \lambda > 0$ Since $T(N_{T2}) < 0$, the existence of N_{T3} follows from the Intermediate Value Theorem.

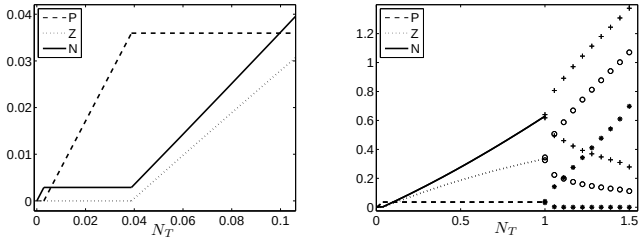

Fig. 3 Steady state values of available nutrient (solid line), phytoplankton (dashed line), and zooplankton (dotted line). When the steady states become unstable, limit cycles occur, and the maximum and minimum values of the periodic orbit are plotted

To prove uniqueness, we show that T is an increasing function of N_T:

$$\frac{dT}{dN_T} = \left(\frac{h(P^*)}{P^*} - h'(P^*)\right) g\frac{dZ^*}{dN_T} - \mu P^* \frac{da}{dN_T}. \tag{35}$$

We now show that this is positive for all N_T by showing that $dZ^*/dN_T > 0$, and $da/dN_T < 0$, since we have assumed $h'(P^*) \geq h(P^*)/P^*$.

The proof that $dZ^*/dN_T > 0$ follows from (18) and the Implicit Function Theorem. Differentiating (18) with respect to N_T yields

$$\frac{dZ^*}{dN_T} = \frac{\gamma\mu P^*}{\delta} f'(N_T - P^* - Z^*)\left(1 - \frac{dZ^*}{dN_T}\right). \tag{36}$$

Rearranging for dZ^*/dN_T and noting that f is increasing yields the result. It can also be seen that $dZ^*/dN_T < 1$.

Now consider $a = f'(N_T - P^* - Z^*)$. Differentiating with respect to N_T yields

$$\frac{da}{dN_T} = f''(N_T - P^* - Z^*)\left(1 - \frac{dZ^*}{dN_T}\right), \tag{37}$$

which is negative since f has negative second derivative, and since $dZ^*/dN_T < 1$. □

Therefore, if $h'(P^*) < h(P^*)/P^*$, there exists a third critical value of total nutrient, N_{T3}, where the equilibrium point (P^*, Z^*) switches from stable to unstable as N_T is increased. Since this value is unique, stability cannot be regained by further increasing the total nutrient. At this value, N_{T3}, there is a Hopf bifurcation. For the parameters in Table 1, numerical simulations suggest that this is a supercritical Hopf bifurcation, where stable periodic orbits exist for $N_T > N_{T3}$. In Figure 3 the steady states are plotted when they are stable, and then the maximum and minimum values of the limit cycles when $N_T > N_{T3}$ are plotted. A similar figure can be found in (Wroblewski et al, 1988), though they do not include stability analysis and they only include equilibrium solutions, not limit cycles.

In Franks et al (1986), numerical simulations using a Type II response produced periodic orbits, while a Mayzaud-Poulet type response, which does not saturate and has positive second derivative, led to stable equilibrium solutions. Consequently, as

pointed out in Gentleman and Neuheimer (2008), it was mistaken that it is the saturation that causes instability, when in truth it is the relation between $h'(P^*)$ and $h(P^*)/P^*$. In fact, the shape of the response for $P > P^*$ is unimportant and the saturation has no effect on a fixed equilibrium point. Since the Mayzaud-Poulet response has positive second derivative, $h'(P^*) \geq h(P^*)/P^*$, the positive equilibrium is always stable. As well, a Type II response will lead to periodic orbits for initial conditions such that $N_T > N_{T3}$, so those numerical results are consistent with our analysis.

In Gentleman and Neuheimer (2008), the authors assume the dissolved nutrient is saturated (i.e. setting $f(N) = 1$) in their analysis, which misses some of the details. For a Type III response, this does not change the analysis, but for a Type II response, it implies that the positive equilibrium is always unstable. This is not true since the destabilizing effects of the zooplankton grazing response can be overcome by the stabilizing process of the nutrient uptake by phytoplankton. That is, the growth rate per unit biomass of phytoplankton decreases with increasing phytoplankton. This is because the more biomass there is within the phytoplankton population, the less biomass there is that is available to be uptaken by phytoplankton, which decreases the growth rate. This stabilizing influence becomes less important as the total biomass in the system increases.

In Ruan (2001), the author analyzes a similar chemostat-type model that includes a washout rate. This model includes nutrient of concentration N^0 flowing in at a rate of D. The parameter N^0 is analogous to our N_T, and the author obtains similar results, including those for the existence and stability of the three different types of equilibrium for different values of N^0. In the chemostat model, for example, the concentration of nutrient must be sufficiently large to sustain the plankton populations. As well, using a Type II response, the author proves the existence of a Hopf bifurcation. These similarities suggest that the amount of biomass in the system plays a significant and consistent role regardless of the specific form of the model equations.

6 Stability of Solutions with Delay

While conserved NPZ models have been studied without delay in nutrient recycling, and non-conservative models have been studied with this delay, to our knowledge, no one has studied a conserved NPZ model with delay in nutrient recycling. We now investigate the effect that the delay in nutrient recycling has on the three different types of equilibrium points. In the case of the trivial equilibrium, the presence of delay does not change the characteristic equation:

$$\det \begin{pmatrix} s & \mu f(N_T) - \lambda \hat{\eta}(s) & -\delta \hat{\eta}(s) \\ 0 & s - \mu f(N_T) + \lambda & 0 \\ 0 & 0 & s + \delta \end{pmatrix} = 0. \tag{38}$$

The requirements for stability are the same as in the case with no delay. That is, the point $(N_T, 0, 0)$ is stable if $N_T < N_{T1}$, and unstable if $N_T > N_{T1}$. In fact, if the trivial equilibrium is stable, it is globally stable, since

$$\frac{d}{dt}(P+Z) = (\mu f(N) - \lambda)P - (1-\gamma)gZh(P) - \delta Z \leq -m(P+Z) \tag{39}$$

where $m = \min(\lambda - \mu f(N_T), \delta) > 0$. This implies that P and Z both asymptotically approach zero, and the conservation law therefore implies that N asymptotically approaches N_T.

The delay does change the characteristic equation for the other two types of equilibrium points. Since the equilibrium points come in lines parameterized by the total nutrient, we will study the stability both in terms of equilibrium values and mean delay, as well as total nutrient and mean delay. First we explore the equilibrium point with no zooplankton.

6.1 Stability of Equilibrium with No Zooplankton

Substituting $(\hat{N}, \hat{P}, 0)$ into A_0 and A_1 yields

$$A_0 = \begin{pmatrix} -\mu\hat{P}a & -\lambda & 0 \\ \mu\hat{P}a & 0 & -gd \\ 0 & 0 & \gamma gd - \delta \end{pmatrix}, \qquad A_1 = \begin{pmatrix} 0 & \lambda & \delta + (1-\gamma)gd \\ 0 & 0 & 0 \\ 0 & 0 & 0 \end{pmatrix}, \tag{40}$$

since $c = f(\hat{N}) = \lambda/\mu$. The characteristic equation is then:

$$\det \begin{pmatrix} s + \mu\hat{P}a & \lambda(1-\hat{\eta}(s)) & -[\delta + (1-\gamma)gd]\hat{\eta}(s) \\ -\mu\hat{P}a & s & gd \\ 0 & 0 & s - \gamma gd + \delta \end{pmatrix}, \tag{41}$$

$$= (s - \gamma gd + \delta)[s^2 + \mu\hat{P}as + \mu\hat{P}a\lambda(1-\hat{\eta}(s))], \tag{42}$$

$$= 0. \tag{43}$$

The root $s = \gamma gd - \delta$ is negative if $N_T < N_{T2}$, where N_{T2} is given by (20). We therefore see the same transcritical bifurcation points N_{T1} and N_{T2} here as we did in the model with no delay. If $N_T < N_{T2}$, stability then depends on the roots of $s^2 + \mu\hat{P}as + \mu\hat{P}a\lambda(1-\hat{\eta}(s))$.

Proposition 4 *If the total biomass, N_T, and the mean delay, τ, are such that*

$$f^{-1}\left(\frac{\lambda}{\mu}\right) + \frac{2\lambda(1+\tau\lambda)}{\mu a} \le N_T < f^{-1}\left(\frac{\lambda}{\mu}\right) + (1+\tau\lambda)h^{-1}\left(\frac{\delta}{\gamma g}\right) \equiv N_{T2}, \tag{44}$$

then $(\hat{N}, \hat{P}, 0)$ is stable.

Proof The inequality $N_T < N_{T2}$ is necessary and sufficient so that the eigenvalue $\gamma gd - \delta$ is negative. Using the definition of $\hat{P}$ in (14) the other inequality can be shown to be equivalent to $2\lambda \le \mu\hat{P}a$. Using Rouché's Theorem (Churchill and Brown, 1984), we now show that if $2\lambda \le \mu\hat{P}a$, then all the non-zero roots of $s^2 + \mu\hat{P}as + \mu\hat{P}a\lambda(1-\hat{\eta}(s))$ have negative real part. This theorem says that if f_1 and f_2 are analytical functions, $|f_1(s)| \ge |f_2(s)|$ on some simple closed contour C, and neither function reduces to zero at any point on C, then $f_1(s)$ and $f_1(s) + f_2(s)$ have the same number of zeros inside C.

Let $f_1(s) = s^2 + \mu\hat{P}as + \mu\hat{P}a\lambda$ and $f_2(s) = -\mu\hat{P}a\lambda\hat{\eta}(s)$. Let the contour $C = C_1 \cup C_2$ be given by

$$C_1: \quad s = Re^{i\theta}, \quad \theta \in \left[-\frac{\pi}{2}, \frac{\pi}{2}\right], \tag{45}$$

$$C_2: \quad s = iy, \quad y \in [-R, R]. \tag{46}$$

We wish to show that $|f_1(s)| \geq |f_2(s)|$ on C. Since $|f_2(s)| \leq \mu\hat{P}a\lambda$ it is sufficient to show that $|f_1(s)|^2 \geq (\mu\hat{P}a\lambda)^2$ on C.

On C_1, $|f_1(Re^{i\theta})|^2 = (R^2\cos 2\theta + \mu\hat{P}aR\cos\theta + \mu\hat{P}a\lambda)^2 + (R^2\sin 2\theta + \mu\hat{P}aR\sin\theta)^2 \geq (\mu\hat{P}a\lambda)^2$, for R sufficiently large.

On C_2, $|f_1(iy)|^2 = (\mu\hat{P}a\lambda - y^2)^2 + (\mu\hat{P}ay)^2$. Under the assumption that $2\lambda \leq \mu\hat{P}a$, a simple computation shows that the minimum value $|f_1(iy)|^2$ takes with respect to y is at $y = 0$. That is, $|f_1(iy)|^2 \geq (\mu\hat{P}a\lambda)^2$. However, if $2\lambda > \mu\hat{P}a$, the minimum value occurs at $y^2 = \mu\hat{P}a(\lambda - \frac{1}{2}\mu\hat{P}a)$, and it can be seen that the value of $|f_1(s)|^2$ at this point is less than $(\mu\hat{P}a\lambda)^2$.

Therefore, if $2\lambda \leq \mu\hat{P}a$, then by Rouché's Theorem, $f_1(s)$ and $f_1(s) + f_2(s)$ have the same number of zeros inside C. Letting $R \to \infty$, the interior of C is the same as the open righthand plane. Since $f_1(s)$ has no roots with positive real parts, $s^2 + \mu\hat{P}as + \mu\hat{P}a\lambda(1 - \hat{\eta}(s))$ also has no roots with positive real parts. □

For this result to be useful, from (44) it is required that $2\lambda/\mu a < h^{-1}(\delta/\gamma g)$. If this is true, then for any $N_T \geq 2\lambda/\mu a$ we can find a range of values for τ such that $(\hat{N}, \hat{P}, 0)$ is stable. In this case, the stability only has delay-dependence through the mean, and the general shape of the distribution does not matter (although we do require that its Laplace transform is analytic in the closed righthand plane).

Using equations (14) and (17), $N_T < N_{T2}$ is equivalent to $\hat{P} < P^*$. From an ecological perspective, Proposition 4 shows that the phytoplankton equilibrium value must be less than that needed to sustain the zooplankton population, otherwise a small amount of zooplankton will grow in time instead of decaying to zero. Additionally, since the other inequality in Proposition 4 is equivalent to $2\lambda \leq \mu\hat{P}a$ the results says that the equilibrium point is stable if the death rate of phytoplankton is sufficiently small compared to the maximum growth rate. Additionally, increasing the equilibrium value of phytoplankton, $\hat{P}$, (as long as $\hat{P} < P^*$ holds) or decreasing the equilibrium value of dissolved nutrient (which increases a: the slope of the phytoplankton uptake functional response at the equilibrium), has a stabilizing effect.

In Jang and Baglama (2005), the authors state a similar result for a model that includes washout rates. They find an inequality that guarantees local asymptotic stability that is independent of the delay distribution for the equilibrium solution without zooplankton. Their result is more complicated because of the nature of their model, but it can be seen to be identical to our condition as the washout rate approaches zero.

We can explore this type of equilibrium further in the case of a discrete delay. Letting $\eta(u) = \delta(u - \tau)$, the characteristic equation becomes

$$(s - \gamma gd + \delta)[s^2 + \mu\hat{P}as + \mu\hat{P}a\lambda(1 - e^{-s\tau})] = 0. \tag{47}$$

Setting the real part of s to zero allows us to solve for possible delays where stability might switch. That is, it gives us values for τ where there are eigenvalues on

the imaginary axis. Substituting $s = i\omega$ into the second factor of the characteristic equation and separating the real and imaginary parts gives the equations:

$$-\omega^2 + \mu\hat{P}a\lambda[1-\cos(\omega\tau)] = 0, \tag{48a}$$

$$\omega + \lambda\sin(\omega\tau) = 0. \tag{48b}$$

From these equations, we can isolate $\cos(\omega\tau) = 1 - \omega^2/(\mu\hat{P}a\lambda)$ and $\sin(\omega\tau) = -\omega/\lambda$. Squaring both sides and adding the equations then yields:

$$\omega^2\left[\omega^2 - 2\mu\hat{P}a\lambda + (\mu\hat{P}a)^2\right] = 0. \tag{49}$$

The zero solution is the inherent one. For other solutions to exist, we require

$$2\lambda > \mu\hat{P}a, \tag{50}$$

since ω is real. Thus, if $2\lambda \leq \mu\hat{P}a$, then no other solutions exist. Therefore changing the value of the delay while keeping $\hat{P}$ fixed cannot move eigenvalues across the imaginary axis. Therefore if the equilibrium point is stable without delay, it remains stable for any value of delay. We emphasize that we are assuming that $\hat{P}$ is fixed while the total biomass increases with the delay. On the other hand, if we assume the total biomass is fixed, then increasing the delay decreases $\hat{P}$, so the equilibrium point remains stable as long as (50) still holds. It can be seen that this is a specific case of Proposition 4.

Otherwise, if $2\lambda > \mu\hat{P}a$ there are critical eigenvalues $s = \pm i\omega_c$, where $\omega_c = \sqrt{2\mu\hat{P}a\lambda - (\mu\hat{P}a)^2}$. Solving for for the corresponding critical delay from (48b) gives:

$$\tau_c = \frac{1}{\omega_c}\sin^{-1}\left(\frac{-\omega_c}{\lambda}\right), \tag{51}$$

with proper care to ensure that the correct solutions are taken. That is, (48a) must be satisfied, so $\cos(\omega_c\tau_c)$ must have the same sign as $1 - \omega_c^2/(\mu\hat{P}a\lambda)$. Another detail is making sure that $\omega_c \leq \lambda$ so that (51) has solutions. In fact, this is always true since

$$\lambda^2 - \omega_c^2 = \lambda^2 - 2\mu\hat{P}a\lambda + (\mu\hat{P}a)^2 = (\lambda - \mu\hat{P}a)^2 \geq 0. \tag{52}$$

Equation (51) can be non-dimensionalized in a useful way. Letting $\hat{\tau}_c = \lambda\tau_c$ and $x = \mu\hat{P}a/\lambda$, we get the following equation for a critical delay:

$$\hat{\tau}_c = \frac{1}{\sqrt{2x - x^2}}\sin^{-1}\left(-\sqrt{2x - x^2}\right), \tag{53}$$

with

$$\cos(\omega_c\tau_c) = 1 - \omega_c^2/(\mu\hat{P}a\lambda), \tag{54}$$

$$= 1 - \frac{1}{x}\frac{\omega_c^2}{\lambda^2}, \tag{55}$$

$$= x - 1. \tag{56}$$

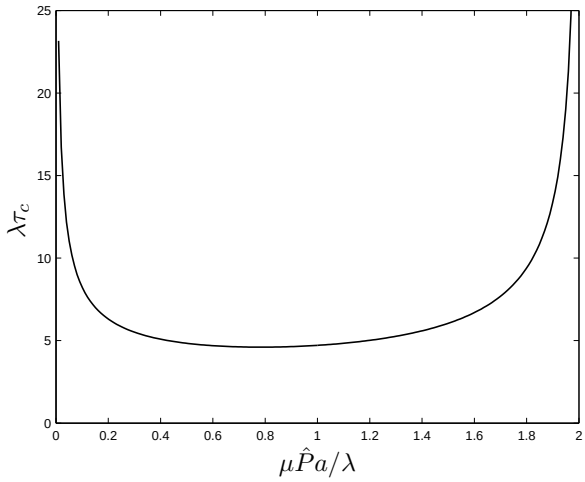

Fig. 4 A plot of non-dimensional critical delay against non-dimensional phytoplankton equilibrium. By inspection of the graph, the minimum value is approximately 4.6, indicating that $\tau_c \geq 4.6/\lambda$

Then, taking the range of the inverse of sine to be in $[-\frac{\pi}{2}, \frac{\pi}{2}]$ we get

$$\hat{\tau}_c = \begin{cases} \frac{1}{\sqrt{2x-x^2}}\left[\pi - \sin^{-1}\left(-\sqrt{2x-x^2}\right)\right] & \text{if } 0 < x \leq 1 \\ \frac{1}{\sqrt{2x-x^2}}\left[2\pi + \sin^{-1}\left(-\sqrt{2x-x^2}\right)\right] & \text{if } 1 < x < 2 \end{cases}. \tag{57}$$

Of course there are other solutions, but we have concerned ourselves with the smallest positive one. A plot of this function is shown in Figure 4. It can be seen from this graph that the minimum value of $\hat{\tau}_c$ is approximately 4.6, which indicates that $\tau_c \geq 4.6/\lambda$. Thus, $\tau < 4.6/\lambda$ is a sufficient condition for local stability when $N_{T1} < N_T < N_{T2}$.

In terms of the original parameters, (57) is

$$\tau_c = \begin{cases} \frac{1}{\omega_c}\left[\pi - \sin^{-1}\left(-\frac{\omega_c}{\lambda}\right)\right] & \text{if } 0 < \mu\hat{P}a \leq \lambda \\ \frac{1}{\omega_c}\left[2\pi + \sin^{-1}\left(-\frac{\omega_c}{\lambda}\right)\right] & \text{if } \lambda < \mu\hat{P}a < 2\lambda \end{cases}, \tag{58}$$

which gives the critical delay for a fixed value of $\hat{P}$. However, we wish to know what the maximum value of the delay is before stability is lost for a given value of total nutrient. This was done for the parameter values in Table 1. In the computation we increase $\hat{P}$ from zero to $2\lambda/(\mu a)$ in small increments. For each $\hat{P}$, τ_c is calculated from (58). Finally, we compute $N_T = f^{-1}(\lambda/\mu) + (1+\lambda\tau_c)\hat{P}$. The results are shown in Figure 5. This figure illustrates regions in the $\tau - N_T$ plane where different behaviour occurs. In this figure, region 1 is stable, meaning $\tau < \tau_c$. This critical delay separates region 1 from region 2. While there may be areas within region 2 that are stable, we did not concern ourselves with them, as any such region would be relatively small

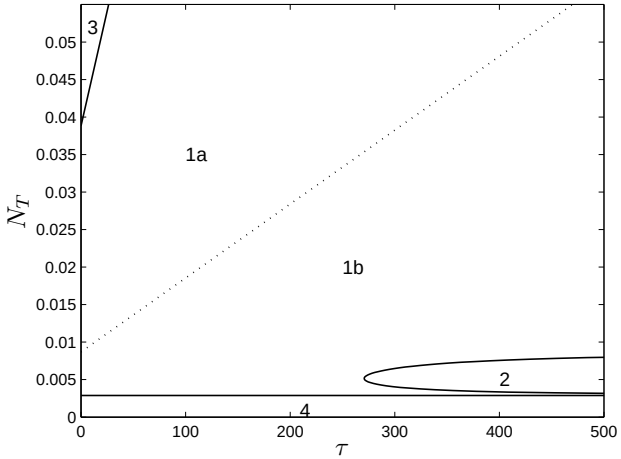

Fig. 5 Regions in the $\tau - N_T$ plane that exhibit different behaviour for the $(\hat{N}, \hat{P}, 0)$ solution. Region 1a is stable regardless of the delay distribution, while region 1b is stable for the discrete delay. Region 3 is unstable. The boundary between region 1 and 2 represents a switch in stability for the model with discrete delay, although there may be areas within region 2 that are stable. Region 4 is where the equilibrium does not exist

in the parameter space and therefore not interesting enough to warrant a more thorough investigation (at least within the context of this paper). Note that $4.6/\lambda \approx 270$, which corresponds to the left-most point of this boundary. Region 3 is unstable, as it corresponds to $N_T > N_{T2}$, where it was shown there is a positive eigenvalue. Region 4 corresponds to the region where the equilibrium does not exist, and the $(N_T, 0, 0)$ solution is stable.

6.2 Stability of Equilibrium with Zooplankton

For the equilibrium (N^*, P^*, Z^*), the characteristic equation is

$$\det \begin{pmatrix} s + \mu P^* a & \mu c - \left(\lambda + \frac{(1-\gamma)\gamma g b P^*(\mu c - \lambda)}{\delta}\right)\hat{\eta}(s) & -\frac{\delta}{\gamma}\hat{\eta}(s) \\ -\mu P^* a & s - \mu c + \lambda + \frac{\gamma g b P^*(\mu c - \lambda)}{\delta} & \frac{\delta}{\gamma} \\ 0 & -\frac{\gamma^2 g b P^*(\mu c - \lambda)}{\delta} & s \end{pmatrix} = 0, \tag{59}$$

where $a = f'(N^*)$, $b = h'(P^*)$, and $c = f(N^*)$. This equation is sufficiently complicated that general analytical results were not found. However, in the case of the discrete delay, where $\hat{\eta}(s) = e^{-s\tau}$, we can make some progress. Substituting in $s = i\omega$ leads to two equations: one such that the real part of the equation is zero, and one such that the imaginary part is. These equations are in the form

$$\mathbf{B}(\omega) \begin{pmatrix} \cos(\omega\tau) \\ \sin(\omega\tau) \end{pmatrix} = \mathbf{y}(\omega), \tag{60}$$

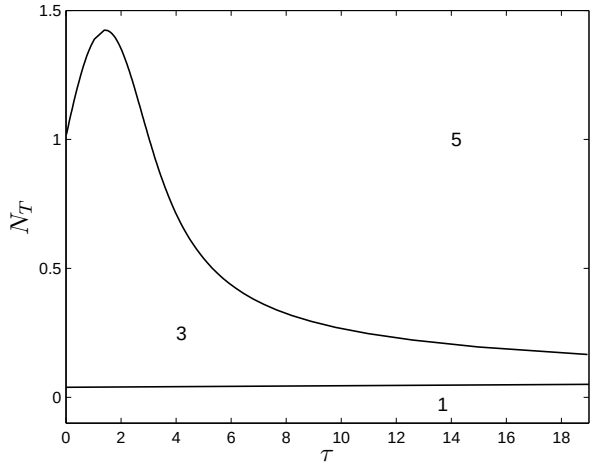

Fig. 6 Regions in the $\tau - N_T$ plane that exhibit different behaviour for the (N^*, P^*, Z^*) solution using the Type II response $h(P) = \frac{P}{P+K}$. Region 1 is where the equilibrium solution does not exist, and where the $(\hat{N}, \hat{P}, 0)$ is stable. Region 3 is where the equilibrium solution exists and is stable, but where $(\hat{N}, \hat{P}, 0)$ is unstable. The curve separating region 3 and region 5 corresponds to an eigenvalue with zero real part, so the assurance of stability is lost in region 5

where $\mathbf{B}$ is a two by two matrix, and $\mathbf{y} \in \mathbb{R}^2$, both with entries that are polynomials in ω. If $\mathbf{x}(\omega) = \mathbf{B}^{-1}(\omega)\mathbf{y}(\omega)$, and x_1 and x_2 are the components of $\mathbf{x}$, then

$$x_1(\omega)^2 + x_2(\omega)^2 = 1, \tag{61}$$

which can then be rearranged into a cubic polynomial in ω^2. The procedure so far can be done symbolically, though it leads to a polynomial with unwieldy coefficients. Consequently we must switch to a numerical approach. Numerically, the roots of the polynomial are easily solved for. Since the polynomial is in ω^2 and ω must be real valued, only positive roots are of concern. If there are no positive roots, there does not exist a critical delay where stability switches. Otherwise, we can obtain for each positive root a value of the delay:

$$\tau_i = \frac{1}{\omega_i} \sin^{-1}(x_2(\omega_i)), \tag{62}$$

with

$$\text{sign}(\cos(\omega_i \tau_i)) = \text{sign}(x_1(\omega_i)), \tag{63}$$

for $i = 1, .., p$, where p is the number of positive roots. The critical delay, τ_c, is then the smallest τ_i.

To compute a curve in the $\tau - N_T$ plane where there is an eigenvalue with zero real part, we begin by increasing N^* in increments from some value slightly larger than N_{T2}. Then τ_c is calculated and then N_T is found from (19) with $\tau = \tau_c$. Figure 6 shows the results of the computation when the functional form of the zooplankton

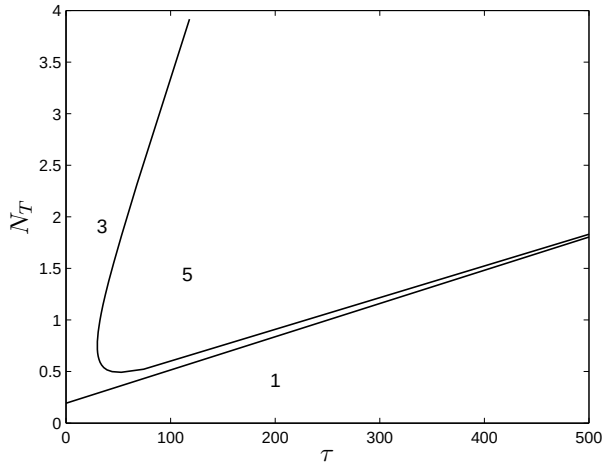

Fig. 7 Regions in the $\tau - N_T$ plane that exhibit different behaviour for the (N^*, P^*, Z^*) solution using the Type III response $h(P) = \frac{P^2}{P^2+K^2}$. Region 1 is where the equilibrium solution does not exist, and where the $(\hat{N}, \hat{P}, 0)$ is stable. Region 3 is where the equilibrium solution exists and is stable, but where $(\hat{N}, \hat{P}, 0)$ is unstable. The curve separating region 3 and region 5 corresponds to an eigenvalue with zero real part, so the assurance of stability is lost in region 5

grazing, $h(P)$, is of Type II. In some cases, it was necessary to compute the two smallest critical delays in order to complete the curve. Region 1 and 3 are the same as before, although from the perspective of the equilibrium solution (N^*, P^*, Z^*) region 1 corresponds to the equilibrium solution not existing, and region 3 is where it exists and is stable. The curve separating region 3 and region 5 indicates where there is a pair of eigenvalues with zero real part, so the assurance of stability is lost in region 5. Interestingly, for some values of total biomass, N_T, we see that the delay can have a stabilizing effect for relatively short delays. After the equilibrium undergoes a Hopf bifurcation at $N_T = N_{Tc} \approx 1$, increasing the delay to an appropriate amount can make the equilibrium stable in some cases.

In Section 5 it was shown that a Type III response can imply that the equilibrium is always stable when there is no delay, so we might expect that increased stability is also present when there is delay. We compute a curve as we did before, but with $h(P) = \frac{P^2}{P^2+K^2}$, which is of Type III. Figure 7 shows the results. It is seen that the delay has to be significantly longer to cause instability in this case when compared to Figure 6 where the functional response was of Type II.

Since the characteristic equation is difficult to handle in a general setting, we consider specific delay distributions. A common class of distributions is the gamma distribution, given by

$$\eta(u) = \frac{u^{p-1}\alpha^p e^{-\alpha u}}{\Gamma(p)}, \tag{64}$$

where p and α are non-negative real numbers and

$$\Gamma(p) = \int_0^\infty u^{p-1} e^{-u}\, du. \tag{65}$$

An attractive feature of this distribution is that its Laplace transform is a rational function:

$$\hat{\eta}(s) = \frac{\alpha^p}{(s+\alpha)^p}. \tag{66}$$

Thus, in the case where p is an integer, the characteristic equation can be rearranged into a polynomial with a finite number of roots. The mean of the distribution function is $\tau = p/\alpha$, so we can replace α in the distribution with p/τ so as to have the mean delay as a parameter. It can be seen that small p values characterize a wider distribution with more variance, while larger p values result in a more narrow distribution. As $p \to \infty$ with τ fixed, η approaches the delta distribution; that is, a discrete delay.

Recall that in the case $p = 1$, the system is equivalent to (6). We then have the following proposition:

Proposition 5 *For the delay distribution $\eta(u) = \alpha e^{-\alpha u}$, if $h'(P^*) \geq h(P^*)/P^*$, then (N^*, P^*, Z^*) is stable when it exists.*

Proof We show that all the roots of the characteristic equation have negative real parts. To make the equation simpler, we define the following quantities: $\hat{a} = \mu P^* a$, $\hat{b} = \mu c - \lambda$, $\hat{c} = \gamma g b P^*/\delta$, and $\hat{d} = \delta/\gamma$. These are all positive numbers. The characteristic equation is then

$$\det \begin{pmatrix} s+\hat{a} & \hat{b}+\lambda-\left(\lambda+(1-\gamma)\hat{b}\hat{c}\right)\frac{\alpha}{s+\alpha} & -\frac{\alpha\hat{d}}{s+\alpha} \\ -\hat{a} & s+\hat{b}(\hat{c}-1) & \hat{d} \\ 0 & -\gamma\hat{b}\hat{c} & s \end{pmatrix} = 0, \tag{67}$$

which implies

$$s(s^3 + c_2 s^2 + c_1 s + c_0) = 0, \tag{68}$$

where

$$c_2 = \alpha - T, \tag{69}$$

$$c_1 = -\alpha T + \gamma\hat{b}\hat{c}\hat{d} + \lambda\hat{a} + \hat{a}\hat{b}\hat{c}, \tag{70}$$

$$c_0 = \alpha\gamma\hat{a}\hat{b}\hat{c} + \alpha\gamma\hat{b}\hat{c}\hat{d} + \gamma\hat{a}\hat{b}\hat{c}\hat{d}, \tag{71}$$

and $T = \hat{b}(1-\hat{c}) - \hat{a}$, which is the trace in (33). The assumption that $h'(P^*) \geq h(P^*)/P^*$ (i.e. $\hat{c} \geq 1$) implies that $T < 0$ and $T + \hat{a} < 0$. The Routh-Hurwitz stability criteria for a cubic polynomial in the present form requires $c_2 > 0, c_1 > 0, c_0 > 0$, and $c_1 c_2 - c_0 > 0$ as necessary and sufficient conditions for all three roots to have negative real part. It can be easily seen that each coefficient is then positive. As well,

$$c_1 c_2 - c_0 = -T\alpha^2 + [T^2 + \lambda\hat{a} + (1-\gamma)\hat{a}\hat{b}\hat{c}]\alpha - (\hat{a}\hat{b}\hat{c} + \lambda\hat{a})T - (\hat{a}+T)\gamma\hat{b}\hat{c}\hat{d}, \tag{72}$$

which is positive. □

This proposition does not apply to Type II responses, since then $h'(P^*) < h(P^*)/P^*$. However, this assumption is not necessary for stability. In the limit as α becomes large, we can see that the Routh-Hurwitz stability criteria is met if and only if $T < 0$, which is the same condition for stability with no delay. This is expected since the mean delay here is $\tau = \alpha^{-1}$.

We can apply a similar analysis to other gamma distributions, but setting $p \geq 2$ in (64) yields much more complicated characteristic equations with increasingly difficult Routh-Hurwitz criteria. Conditions for stability obtained from looking at the characteristic equation symbolically are less likely to be meaningful as the expressions get complicated. As well, we would like to consider other types of distributions with less pleasant Laplace transforms, so we will turn to numerical methods.

We now introduce two other types of distributions. The first is the uniform distribution, which will be defined as:

$$\eta(u) = \begin{cases} \frac{1}{2W}, & \tau - W \leq u \leq \tau + W \\ 0, & \text{elsewhere} \end{cases}, \tag{73}$$

where $\tau \geq W$ is the mean delay. The variance of this distribution is $V = W^2/3$.

The second distribution to be considered is what we will refer to as the "tent" distribution:

$$\eta(u) = \begin{cases} \frac{u+W-\tau}{W^2}, & \tau - W \leq u \leq \tau \\ \frac{-u+W+\tau}{W^2}, & \tau \leq u \leq \tau + W \\ 0, & \text{elsewhere} \end{cases}. \tag{74}$$

Again, $\tau \geq W$ is the mean delay. The variance is $V = W^2/6$.

As well, it can be seen that the mean delay of the gamma distribution (64) is $\tau = p/\alpha$, and the variance is $V = p/\alpha^2$. Figure 8 shows these three distributions, with the same mean delay, and the same variance.

The goal now is to find curves in the $\tau - N_T$ plane where the characteristic equation has roots with zero real part. The characteristic equation is obtained by finding the Laplace transform of the distribution of interest and substituting it into (59). Then we set the real part of the roots to zero by making the substitution $s = i\omega$. Separating the resulting equation into real and imaginary parts yields two equations in three variables: ω, τ, and N^*. These equations describe curves in the $\tau - N^*$ plane that are parameterized by ω. Using pseudo-arclength continuation, as described in (Govaerts, 2000), we can compute points $(\omega_i, \tau_i, N_i^*)$ that satisfy the two equations. Then we can transform each (τ_i, N_i^*) into (τ_i, N_{Ti}) through equation (19) and plot the results.

For this method to work, we need to start near a solution. If the mean delay is close enough to zero, then the solutions should be close to that when there is no delay. This gives a good initial guess. This is not a problem for the gamma distribution, since for any given variance, the mean delay can be arbitrarily small. However, in the cases of the uniform and "tent" distributions, the mean delay cannot be made close to zero unless the variance is also small. To deal with this, in the case of the uniform distribution, we introduce a similar class of distributions:

$$\eta(u) = \begin{cases} \frac{1}{2\tau}, & 0 \leq u \leq 2\tau \\ 0, & \text{elsewhere} \end{cases}. \tag{75}$$

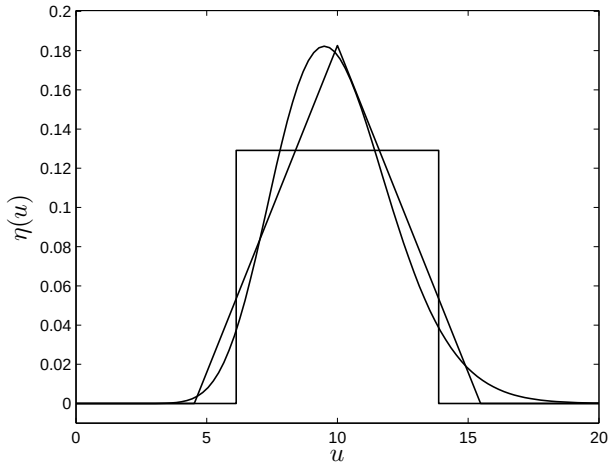

Fig. 8 The uniform, "tent", and gamma distributions with mean delay $\tau = 10$ and variance $V = 5$

Here the mean delay can be made arbitrarily small so there is no problem finding a starting point. Furthermore, the curve of solutions found using this distribution defines appropriate starting points for the uniform distribution (73) by beginning at $\tau = W$. A similar approach can be used for the "tent" distribution with:

$$\eta(u) = \begin{cases} \frac{u}{\tau^2}, & 0 \le u \le \tau \\ \frac{-u+2\tau}{\tau^2}, & \tau \le u \le 2\tau \\ 0, & \text{elsewhere} \end{cases}, \tag{76}$$

Figures 9 and 10 show the curves obtained using this approach for the uniform and "tent" distributions respectively. The figures show the curves in both the $\tau - N^*$ and $\tau - N_T$ planes. The stable region is located below the curve and the unstable region above. Comparing these figures with Figure 6 for small τ, it can be seen that the curves are very similar. This is to be expected since these distributions have small variance when the mean delay is small, so we expect the behaviour to be similar to that of a discrete delay. When the mean delay is larger, however, differences become apparent. The most important difference is that the region of stability becomes larger in the case of a distributed delay. From equation (19) it can be seen that if N^* is constant, then N_T is a linear function of τ, which explains the slope upwards in the N_T case when the curve levels off for N^*. Since N_T is the more meaningful parameter, we will only show plots in the $\tau - N_T$ plane for the remainder of the manuscript, but the transformation from equation (19) should be kept in mind when interpreting such curves. That is, if N_T is fixed, then an increase in the average delay means a decrease in the equilibrium value of nutrient in the water. Or, equivalently, for a fixed amount of nutrient in equilibrium, an increase in the delay means an increase of total nutrient in the system.

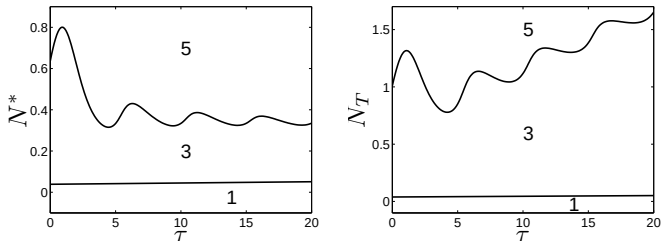

Fig. 9 Stability regions for the uniform distribution defined in (75). Regions 1,3, and 5 are as described in Figure 6

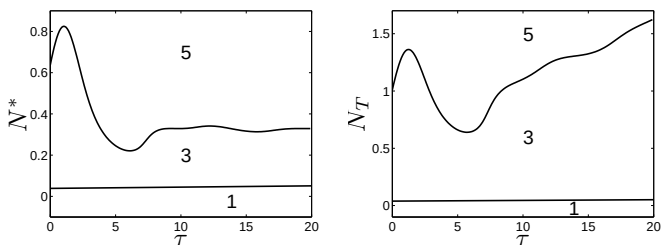

Fig. 10 Stability regions for the uniform distribution defined in (76). Regions 1,3, and 5 are as described in Figure 6

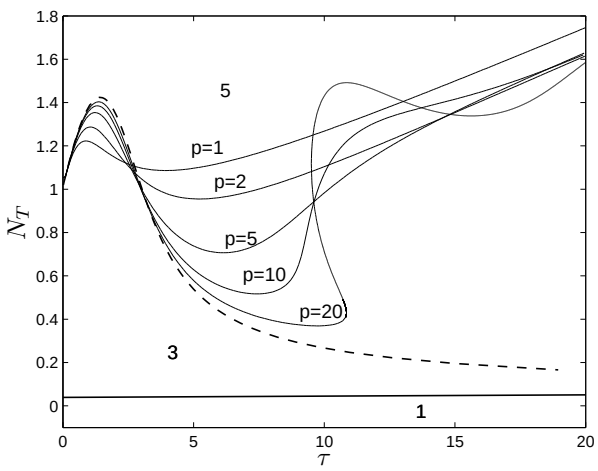

Fig. 11 Stability regions for gamma distributions with fixed p. The dotted line corresponds to the stability region in the case of the discrete delay. Regions 1,3, and 5 are as described in Figure 6

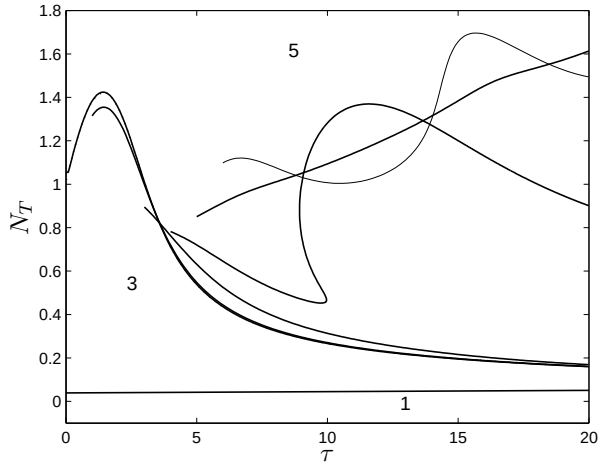

Fig. 12 Stability regions for uniform distributions with various widths. Regions 1,3, and 5 are as described in Figure 6. The starting point of the curve represents the value of W in (73). The values here are $W = 0.001, 1, 3, 4, 5, 6$. Also plotted is the stability region for the discrete delay, although it is almost identical to the uniform distribution with $W = 0.001$ and therefore is hard to see

Figure 11 shows the stability regions for various gamma distributions where p is fixed. Here and in the figures that follow, region 1 corresponds to where the equilibrium point does not exist. Region 3 corresponds to where the equilibrium is stable and its boundary is defined by the appropriate curve, and region 5 corresponds to where it is possibly unstable. Increasing the value of p, which corresponds to making the distribution more narrow, appears to have a slightly stabilizing effect for small mean delays, but has a much greater destabilizing effect for mean delays in the range of about 4-10 days. For example, if the mean delay is 8 days, then the total nutrient must be significantly less if $p = 20$ than if $p = 1$. The behaviour is less clear for mean delay larger than approximately 10 days, though the effect of changing p seems to be less significant as τ gets large.

Figure 12 shows the stability regions for uniform distributions with different widths. It can be seen that these are very similar to the stability region of the discrete delay for W up to 3. However, at $W = 4$ we see a qualitative change in that the curve begins to oscillate. We will discuss why this might be true later. The trend that a wider distribution is less stable for small mean delays, and more stable for larger mean delays continues here.

Figure 13 shows the stability regions for the "tent" distributions with different widths. The characteristics of these curves are very similar to those for the uniform distribution. For W up to 5, the curves are very similar to that for the discrete delay, and for $W = 6$ and above we see a qualitative change.

More precisely, this qualitative change occurs at about $W = 3.95$ in the uniform case and $W = 5.65$ in the "tent" case. At these points, the variance of the uniform distribution is $V = W^2/3 = 5.20$ and in the "tent" distribution it is $V = W^2/6 =$

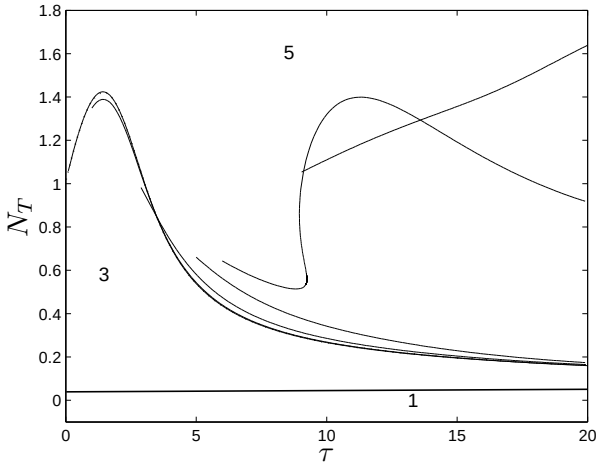

Fig. 13 Stability regions for "tent" distributions with various widths. Regions 1,3, and 5 are as described in Figure 6. The starting point of the curve represents the value of W in (74). The values here are $W = 0.001, 1, 3, 5, 6, 7$. Also plotted is the stability region for the discrete delay, although it is almost identical to the "tent" distribution with $W = 0.001$ and therefore is hard to see

5.32. The variances are very similar, which might be an indication that the curves depend more on the variance than the actual shape. Hence the distributions were reparameterized in terms of their mean delay and variance so that more meaningful comparisons can be made.

Figure 14 shows the curve of solutions where an eigenvalue has zero real part for the gamma, uniform, and "tent" distributions where the variance is fixed at 1 day^2. Also shown for comparison is the curve defining the stability region for the discrete delay. The curves for the three distributed delays are almost identical where they are defined. Furthermore, they are very similar to the curve for the discrete delay, especially for longer mean delays. For short delay, the region of stability is smaller for the distributed delays than it is for the discrete delay, while the opposite is true for longer delays.

Figure 15 shows the same curves as in Figure 14, but where the variance is 5 day^2. We can see more variation among the distributed delays, though they are still very similar where they are defined. The difference between the distributed delays and the discrete delay is more pronounced here. We still see that for short delay, the stability region is larger in the case of discrete delay, while it is larger for the distributed delays for longer mean delays.

Figure 16 shows the case when the variance is 8 day^2. We see even more variation among the distributed delays and it can no longer be said that the three curves are similar. The distributed delay curves are now much different than the discrete delay curve, but we still see that the discrete delay is more stable at smaller mean delays while the distributed delay is more stable for longer mean delays.

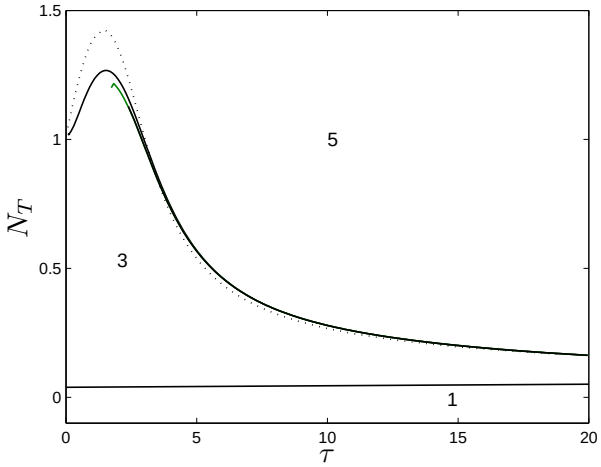

Fig. 14 Stability regions for the gamma, uniform, and "tent" distributions where the variance is fixed at 1 day^2. Regions 1,3, and 5 are as described in Figure 6. Here the curves are almost identical in the three cases. The dotted line represents the curve in the case of the discrete delay and the line at the bottom is the line above which the equilibrium exists

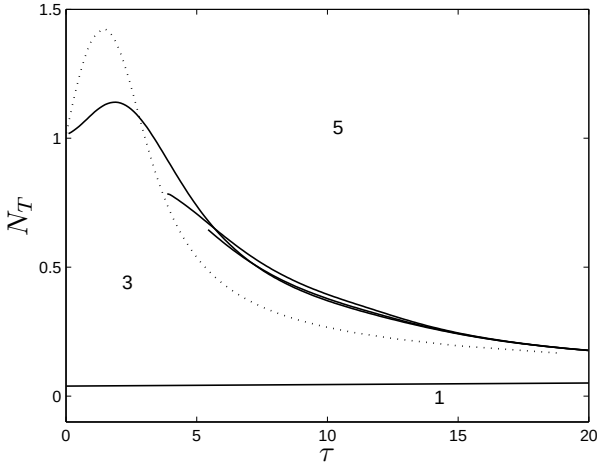

Fig. 15 Stability regions for the gamma, uniform, and "tent" distributions where the variance is fixed at 1 day^2. Regions 1,3, and 5 are as described in Figure 6. The curve for the gamma distribution starts close to $\tau = 0$ while the curve for the "tent" distribution starts the furthest right. The dotted line represents the curve in the case of the discrete delay and the line at the bottom is the line above which the equilibrium exists

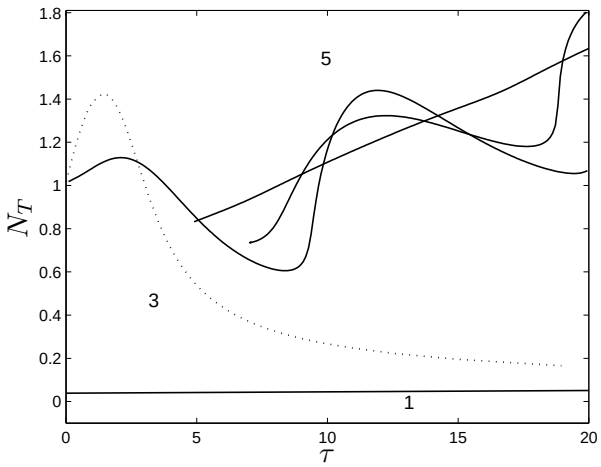

Fig. 16 Stability regions for the gamma, uniform, and "tent" distributions where the variance is fixed at 1 day^2. Regions 1,3, and 5 are as described in Figure 6. The curve for the gamma distribution starts close to $\tau = 0$ while the curve for the "tent" distribution starts the furthest right. The dotted line represents the curve in the case of the discrete delay and the line at the bottom is the line above which the equilibrium exists

7 Simulations

The stability results were verified with a number of simulations. Using the parameter values in Table 1. Solutions were found using MATLAB's built in functions *ode45* and *dde23* for the cases of no delay and discrete delay, respectively. For distributed delays, a custom-made second order scheme was used to solve the equations. This scheme included the numerical integration of the convolution in (1) using the trapezoidal rule and the time-stepping was done using a second order method so overall the method has second order accuracy. We tested the accuracy of this scheme on toy problems with exact solutions, and also on the full problem with the gamma distribution, which can be compared with the solution of the equivalent system of ODE's.

Figure 17 shows some phase portraits in the case with no delay for various values of total nutrient. The behaviour of the solutions in this figure are consistent with the results in Figure 3. Furthermore, at least for the parameter values being used, the equilibrium points appear to be globally asymptotically stable when they are stable. This global stability might be interesting to investigate in the future.

To verify the stability of equilibrium solutions with delay, for a given distribution we choose values of N_T and τ, then compute the corresponding equilibrium point. The initial conditions for the simulation are then chosen to be a small perturbation

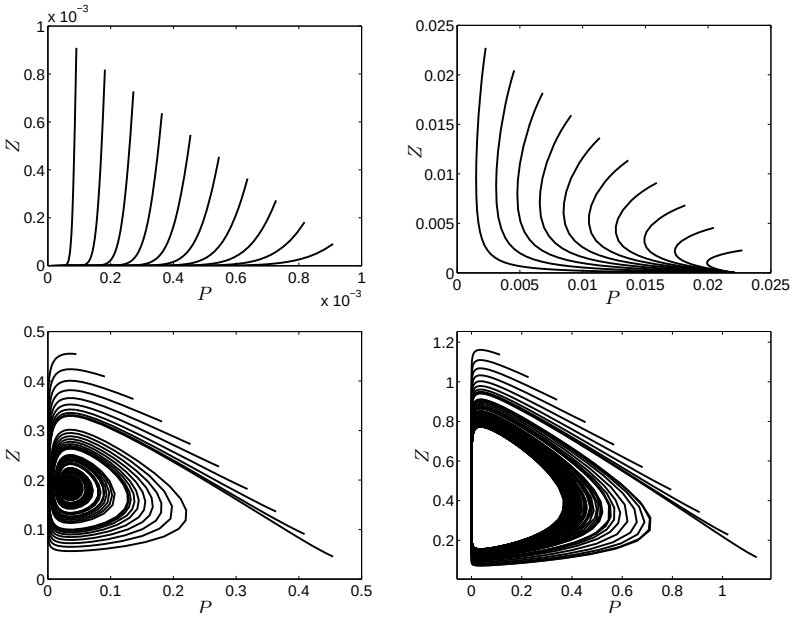

Fig. 17 Simulations of equations (28) with initial conditions on the line $P+Z=N_T$. The top left is for $N_T=0.001<N_{T1}$. The top right is for $N_{T1}<N_T=0.025<N_{T2}$. The bottom left is for $N_{T2}<N_T=0.5<N_{T3}$. The bottom right is for $N_{T3}<N_T=1.25$

from this equilibrium solution that preserves the total nutrient. For example

$$N(t)=N_T-(P^*+\varepsilon)-Z^*-[\lambda(P^*+\varepsilon)+\delta Z^*+(1-\gamma)gZ^*h(P^*+\varepsilon)]\tau, \quad (77)$$

$$P(t)=P^*+\varepsilon, \quad (78)$$

$$Z(t)=Z^*, \quad (79)$$

for $t\in[-r,0]$ where r is the maximum delay being considered [1] and ε is a small number. It was assumed that the equilibrium solution was stable if the resulting oscillations decayed in time, and unstable if they grew. While this is not a rigourous conclusion by itself, the fact that all the simulations we performed agreed with the stability analysis in the previous sections serves as a good check that our methods were correct.

For example, in Figure 18, four simulations are shown using the gamma distribution with $p=20$. The top left is for total nutrient $N_T=0.5$ and mean delay $\tau=5$, and indicates that the equilibrium solution is stable. The top right increases the mean delay to $\tau=8$ and keeps the total nutrient at $N_T=0.5$, and indicates instability. The bottom left is still for $N_T=0.5$, and with the mean delay increased further to $\tau=12$, and suggests a return to stability. Finally, the bottom right is for the total nutrient decreased to $N_T=0.4$ and the mean delay at $\tau=8$. This indicates stability, although

[1] In the case where the delay distribution extends infinitely into the past, the delay distribution must be approximated by a truncated version for simulation purposes.

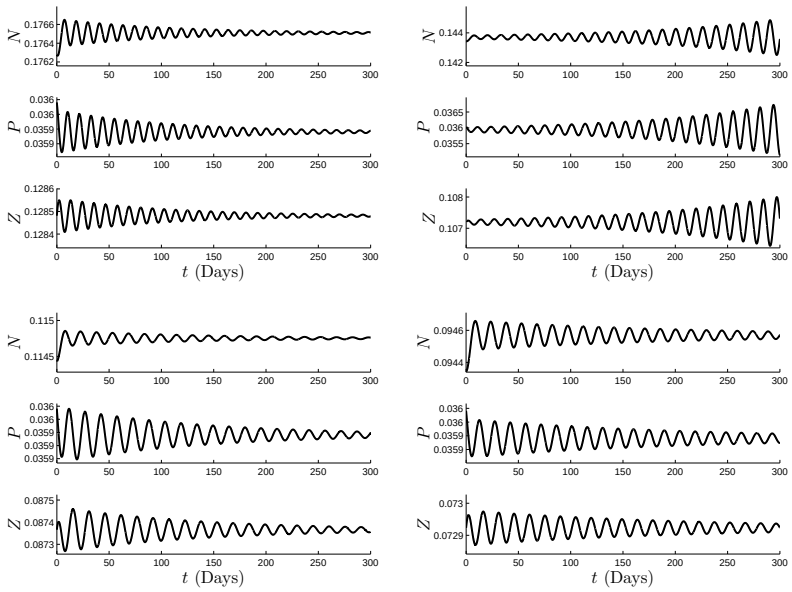

Fig. 18 Simulations for the gamma distribution with $p = 20$. The top left is for total nutrient $N_T = 0.5$ and mean delay $\tau = 5$. The top right is for $N_T = 0.5$ and $\tau = 8$. The bottom left is for $N_T = 0.5$ and $\tau = 12$. The bottom right is for $N_T = 0.35$ and $\tau = 8$

it was unstable for a larger value of total nutrient and the same mean delay. This transient behaviour agrees with the stability regions in Figure 11. Similar tests were done on with other distributions for other values of total nutrient and mean delay, and no inconsistencies with the analysis were found.

8 Discussion

We have looked at a simple ecosystem governed by delay differential equations in order to study how the existence and stability of equilibrium solutions depend on the quantity of nutrient in the system and the delay characterizing the process of nutrient recycling. While our equations were relatively simple, they do offer insight into plankton communities. They verified that a sufficient quantity of biomass is needed in the system in order to sustain a given trophic level. When an additional trophic level has sufficient nutrient to avoid extinction, the equilibrium solution that excludes that species becomes unstable. We see that if the nutrient recycling is characterized by a longer delay, then there is effectively less nutrient in the system that is used to sustain the populations. Therefore, the longer the delay, the more nutrient is needed in the system to sustain a population.

The stability of the equilibrium solution depends on both the amount of biomass in the system, and the properties of the delay distribution. Our computations show this relationship can be complicated, since for a fixed amount of biomass, increasing

the delay can change the stability of an equilibrium solution, sometimes switching it from unstable to stable, or vice versa. This effect was seen mostly in the case of a Type II response for zooplankton grazing on phytoplankton, suggesting a relatively narrow range of values for total nutrient and mean delay where the equilibrium solution is stable. In contrast, a Type III response led to a very robust range of these parameter values where the equilibrium solution is stable, which makes the choice of this response a very important factor when modelling. Further discussion on the importance of this functional response is in (Gentleman et al, 2003), where the authors discuss different functional responses for zooplankton grazing and provide criteria that modelers can use to choose appropriate functional forms.

While our computations primarily focused on a Type II grazing response, this should not be an indication that this type of response is more significant than Type III. In the case of no delay, the system with a Type III response was always stable, and results suggest that the system only becomes unstable for relatively large delays, so this case did not warrant detailed analysis. In fact, the robust stability of the Type III response might lead one to believe it is more realistic than the Type II response, so our focus on the latter should not suggest a preference.

With the mortality rate of $\delta = 0.17$ day^{-1} in Table 1 that was used for our computations, we can place the time scale of the ecosystem at about 6 days. From Figure 6, it can be seen that a typical critical delay value is also of this order. This agrees with the result in (May, 1973), which says that such critical delays are on the same time scale as that of the ecosystem. While this appears to be true for the Type II functional response, Figure 7 suggests that this idea might not be true for a Type III response. In (Edwards, 2001), the author quotes breakdown rates of dead organic matter to be in the range of 0.004-0.2 day^{-1}, placing a typical delay time between 5 and 250 days. For the parameters used in Figures 6 and 7 (see Table 1) This would make the system with a Type II response unstable in most cases, and a Type III response stable for delays on the shorter side of this range. However, different species may have different parameter values than what we have used, so more parameter sets need to be investigated before general comparisons can be made. Nevertheless, we expect the qualitative shape of the stability region to be similar to those seen in Figures 6 and 7, regardless of the parameter values.

There are many other extensions to this work that could be considered. For instance, we could see how the existence and stability of the positive equilibrium is affected by using a nonlinear closure term. We could also investigate other functional responses for zooplankton grazing on phytoplankton, such as a non-monotonic response (Zhu et al, 2002), (Ruan and Xiao, 2001). As well, delay can be incorporated into other terms, such as the gestation time.

The global stability of the positive equilibrium remains to be determined. In the case of instantaneous nutrient recycling, the simulations in the bottom left of Figure 17 suggest that the positive equilibrium is indeed globally asymptotically stable when it is asymptotically stable. However, this might not be true for all parameter values. The global asymptotic stability may be determined via a Lyapunov function or by proving that periodic orbits do not exist as in (van den Driessche and Zeeman, 1998). The global stability of the positive equilibrium in the delayed system could possibly be proved with a Lyapunov functional. In (He and Ruan, 1998), the authors use

Lyapunov functionals to provide conditions for global stability in a two-compartment chemostat model that includes a delay in nutrient recycling and in the gestation time.

Further structure can be added to the model by considering different size classes of plankton, as in (Poulin and Franks, 2010), (Armstrong, 1994), and (Armstrong, 1999). It may be more realistic for the parameters to have size-dependence, and thus it would be interesting to see how the delay in nutrient recycling affects such ecosystems.

Acknowledgements The authors gratefully acknowledge financial support from the Natural Sciences and Engineering Research Council of Canada. M.K. also gratefully acknowledges financial support from the Ontario Graduate Scholarship Program.

References

Armstrong RA (1994) Grazing limitation and nutrient limitation in marine ecosystems: Steady state solutions ofan ecosystem model with multiple food chains. Limnol and Oceanogr 39(3):597–608

Armstrong RA (1999) Stable model structures for representing biogeochemical diversity and size spectra in plankton communities. J Plankton Res 21(3):445–464

Beretta E, Bischi GI, Solimano F (1990) Stability in chemostat equations with delayed nutrient recycling. J Math Biol 28:99–111

Caswell H, Neubert MG (1998) Chaos and closure terms in plankton food chain models. J Plankton Res 20(9):1837–1845

Churchill RV, Brown JW (1984) Complex Variables and Applications. McGraw-Hill, New York

Diekmann O, Gyllenberg M (2012) Equations with infinite delay: Blending the abstract and the concrete. J Differential Equations 252:819–851

van den Driessche P, Zeeman ML (1998) Three-dimensional competitive Lotka-Volterra systems with no periodic orbits. SIAM J Appl Math 58(1):227–234

Edwards AM (2001) Adding detritus to a nutrient-phytoplankton-zooplankton model: a dynamical-systems approach. J Plankton Res 23(4):389–413

Franks PJS (2002) NPZ models of plankton dynamics: Their construction, coupling to physics, and application. J Oceanogr 58:379–387

Franks PJS, Wroblewski JS, Flierl GR (1986) Behavior of a simple plankton model with food-level acclimation by herbivores. Mar Biol 91:121–129

Gentleman W, Leising A, Frost B, Strom S, Murray J (2003) Functional responses for zooplankton feeding on multiple resources: a review of assumptions and biological dynamics. Deep-Sea Res II 50:2847–2875

Gentleman WC, Neuheimer AB (2008) Functional responses and ecosystem dynamics: how clearance rates explain the influence of satiation, food-limitation and acclimation. J Plankton Res 30(11):1215–1231

Govaerts WJF (2000) Numerical Methods for Bifurcations of Dynamical Equilibria. SIAM, Philadelphia

Hale JK, Somolinos AS (1983) Competition for fluctuating nutrient. J Math Biol 18:255–280

He XZ, Ruan S (1998) Global stability in chemostat-type models with delayed nutrient recycling. J of Math Biol 37:253–271

Hino Y, Murakami S, Naito T (1991) Functional Differential Equations with Infinite Delay. Springer-Verlag, Berlin

Holling CS (1966) The functional response of invertebrate predators to prey density. Mem Entomol Soc Can (48):1–86

Jang SRJ, Baglama J (2005) Nutrient-plankton models with nutrient recycling. Comp Math Appl 49:375–387

Kmet T (1996) Material recycling in a closed aquatic ecosystem. ii. bifurcation analysis of a simple food-chain model. Bull Math Biol 58(5):983–1000

Kolmanovskii V, Myshkis A (1999) Introduction to the Theory and Applications of Functional Differential Equations. Kluwer Academic Publishers, Dordrecht

Levin BR, Stewart FM, Chao L (1977) Resource-limited growth, competition, and predation: A model and experimental studies with bacteria and bacteriophage. Am Nat 111(977):3–24

May RM (1973) Time-delay versus stability in population models with two and three trophic levels. Ecol 54(2):315–325

Murray JD (1989) Mathematical biology. Springer-Verlag, Berlin

Poulin FJ, Franks PJS (2010) Size-structured planktonic ecosystems: Constraints, controls and assembly instructions. J Plankton Res 32(8):1121–1130

Ruan S (1998) Turing instability and travelling waves in diffusive plankton models with delayed nutrient recycling. IMA J Appl Math 61:15–32

Ruan S (2001) Oscillatons in plankton models with nutrient recycling. J Theor Biol 208:15–26

Ruan S, Xiao D (2001) Global analysis in a predator-prey system with nonmonotonic functional response. SIAM J Appl Math 61(4):1445–1472

Ulanowicz RE (1972) Mass and energy flow in closed ecosystems. J Theor Biol 34:239–253

Wroblewski JS, Sarmiento JL, Flierl GR (1988) An ocean basin scale model of plankton dynamics in the North Atlantic 1. solutions for the climatological oceanographic conditions in May. Glob Biogeochem Cycles 2:199–218

Zhu H, Campbell SA, Wolkowicz GSK (2002) Bifurcation analysis of a predator-prey system with nonmonotonic functional response. SIAM J Appl Math 63(2):636–682